Novel Push−Pull Phthalocyanines as Targets for Second-Order Nonlinear Applications

Eva M. Maya,[†] Eva M. García-Frutos,[†] Purificación Vázquez,[†] Tomás Torres,*[,†] Guillermo Martín,[‡] Gema Rojo,[‡] Fernando Agulló-López,*[,‡] Raúl H. González-Jonte,[§] Victor R. Ferro,[§] José M. García de la Vega,*[,§] Isabelle Ledoux,*[,||] and Joseph Zyss[||]

Departamento de Química Orgánica (C-I), Departamento de Física de Materiales (C-IV), and Departamento de Química-Física Aplicada (C-XIV), Universidad Autónoma de Madrid, 28049-Madrid, Spain, and Laboratoire de Photonique Quantique et Moléculaire, Ecole Normale Supérieure de Cachan, 94235 Cachan, France

Received: July 31, 2002; In Final Form: January 13, 2003

The second harmonic generation (SHG) hyperpolarizabilities of a family of peripherally substituted push−pull phthalocyanines **1**, **2**, and **3**, having an ethynediyl subunit in the linking bridge between the acceptor and donor moieties, have been measured. Electric field induced second harmonic (EFISH) generation experiments at 1.064 and 1.900 μm and hyper-Rayleigh scattering (HRS) experiments at 1.064 μm have been carried out. The quadratic hyperpolarizabilities values derived from these experiments are quite significant and superior to those found for similar push−pull compounds lacking of a triple C-bond in the donor−acceptor path. The main electronic parameters of the three compounds (electric dipole moments, orbital electronic distributions, and optical transition moments) have been calculated using the ZINDO/S method for molecular geometries that have been optimized through the PM3 method. Excellent agreement with spectroscopic data has been achieved. The SHG results have been analyzed through a 3-level model associated to the ground level and two split levels responsible for the Q-band, assuming either strict (for compound **2**) or approximate (for compounds **1** and **3**) C_{2v} planar symmetry. The parameters used in the model were those obtained from the electronic calculations. For molecule **2**, both the theoretical diagonal and off-diagonal elements of the beta tensor, as well as β_{EFISH} and β_{HRS}, have been determined. Good agreement with the experimental HRS values is obtained, whereas EFISH values considerably differ from those obtained from the simple expression for γ_{EFISH} ignoring the electronic contributions.

Introduction

The rational design of new organic materials for nonlinear optics (NLO) represents a relevant and expanding topic that is reaching maturity because of their potential application in optoelectronics, particularly for the development of optical communications and computing technologies.[1] Second-order, as well as third-order, processes are required for that objective. Although pioneering work has been concentrated on push−pull linear (1D) compounds more complex molecules (both 2D and 3D) and nonlinear mechanisms are being now actively investigated.[2] In other words, the field has strongly diversified and many different design strategies are being followed, including octupolar compounds[2a−f] and nonclassical chromophores.[2g−i] A very interesting family of compounds for this goal is constituted by the phthalocyanines (Pcs).[3] They exhibit excellent thermal and chemical stabilities and offer the possibility of tailoring their physical response due to their remarkable structural versatility.

From the electronic point of view, phthalocyanines are highly conjugated planar molecules with an extensive delocalized π-electron system, which exhibits high cubic hyperpolarizabilities, as well as good optical limiting capabilities.[4] The 2-D structure of Pcs adds some novel features to the SHG response with regard to the behavior found for the more extensively investigated 1D compounds. Nonzero off-diagonal hyperpolarizabilities appear in 2D systems that enhance the versatility of their nonlinear perfomance and, in particular, permit a tuning of the balance between the dipolar and octupolar contributions. Moreover, the higher dimensionality introduces additional complexity that poses new challenges to the theoretical modeling of the SHG response. On the other hand, the potential of phthalocyanine related compounds for second-harmonic generation (SHG) have been recently pointed-out, and different strategies have been developed for obtaining noncentrosymmetric systems. One of them involves the preparation of intrinsically unsymmetric Pc derivatives, such as triazolephthalocyanines,[5] subphthalocyanines (SubPcs),[6] axially substituted Pcs,[7] and other kinds of noncentrosymmetric Pc systems,[8] which have yielded high susceptibility values in both solutions and spin-coated films. As an alternative, it has been suggested that unsymmetrical peripherally substituted Pcs with suitable donor and acceptor groups should exhibit strong second-order nonlinear optical (NLO) responses.[9] They can be considered as push−pull systems mediated by the highly conjugated phthalocyanine macrocycle as a bridging group. Their chemical

* To whom correspondence should be addressed. E-mail addresses: tomas.torres@uam.es; fal@uam.es; delavega@uam.es; ledoux@Ipqm.ens-cachan.fr.

[†] Departamento de Química Orgánica (C-I), Universidad Autónoma de Madrid.

[‡] Departamento de Física de Materiales (C-IV), Universidad Autónoma de Madrid.

[§] Departamento de Química-Física Aplicada (C-XIV), Universidad Autónoma de Madrid.

[||] Ecole Normale Supérieure de Cachan.

10.1021/jp026653e CCC: $25.00
Published on Web 03/04/2003

versatility allows the introduction of many different substituent groups at peripheral positions. However, only a limited number of promising results[8−12] has been derived so far from this strategy, and the experimental studies performed on some asymmetrical Pcs have yielded rather weak values of hyperpolarizabilities. Moreover, the relationship between the second-order response and the molecular structure remains mostly unexplored. Recently, this strategy has been strongly stimulated by work on push−pull arylethynyl porphyrins exhibiting large first-order hyperpolarizabilities.[13] Moreover, successful theoretical proposals to understand and optimize the beta values in highly conjugated push−pull chromophore structures have been advanced.[14] The important role of the topology and electronic structure of the conjugated bridge connecting the donor and acceptor groups has been pointed out. Ideally, the bridge-localized excited state should dramatically alter the D−A coupling relative to the ground state.

In this paper, we describe the second-order NLO properties of a new family of push−pull nitrophenylethynyl- and dimethylaminoethynylphthalocyanines **1**−**3**[15] with extended conjugation, using triple bonds as linkers[16] between the acceptor and donor moieties[14] (see Chart 1). Butoxy and propylsulfonyl substituents in compounds **1**−**3** (as donor and acceptor, respectively) not only promote the required electronic effect but also provide the phthalocyanines with enough solubility in organic solvents to facilitate the preparation of homogeneous thin films. Compounds **1** and **2** having the NO_2 acceptor substituent and the *n*-butoxy donor groups are analogous to the promising push−pull Pcs reported in a recent work[17] (showing moderate hyperpolarizabilities) except for the presence of the triple bond linkage. Therefore, the role of the extended bridge connecting the acceptor group and the Pc macrocycle can be investigated and optimization routes can be explored. Compound **3** having the $N(CH_3)_2$ donor group and the $SO_2C_3H_7$ acceptor has been also studied for comparison purposes.

To have a good understanding of the electronic structure of our molecules, theoretical calculations have been performed to optimize the molecular geometry and determine the relevant frontier orbitals that contribute to the NLO response. Permanent dipole moments as well as optical transition moments have also been obtained. Calculations agree well with the experimental spectroscopic data.

Some relevant features in the experiments and in the analysis of the data are presented in this paper. Hyper-Rayleigh scattering (HRS)[18] measurements have been performed at 1.064 μm together with electric field induced second harmonic (EFISH) generation experiments[19] at two different wavelengths (1.064 and 1.900 μm). The molecule **2**, displaying strict C_{2v} symmetry, has been analyzed in detail within a three-level model[20] including the ground state and the two-split levels of the Q-band transition. A similar analysis for compounds **1** and **3**, assuming an approximate C_{2v} symmetry, yields much poorer results. The three nonzero components of the beta tensor have been determined as well as β_{EFISH} and β_{HRS} by using the electronic molecular parameters obtained from the semiempirical calculations and the measured transition dipole moments between the ground and excited states. The comparison of the HRS experimental data with the theoretical values provides a good test for the adequacy of our model. The EFISH data considerably differ from those directly obtained from the experimental γ_{EFISH}, ignoring the electronic third-order contributions. This discrepancy may be associated to a nonnegligible electronic contribution in our highly conjugated molecules.

CHART 1

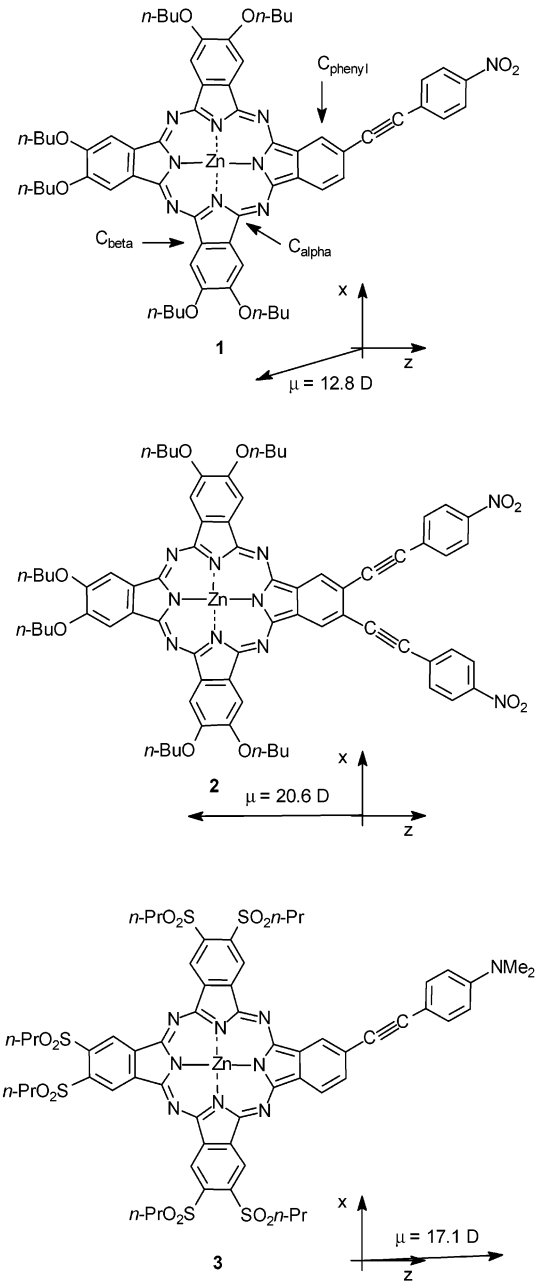

Experimental Section

Synthesis. Compounds **1**−**3**, previously described by us,[15] were prepared by a stepwise method combining a metal template cyclotetramerization and a cross-coupling palladium mediated reaction.

EFISH Generation Measurements. EFISH experiments have been performed in chloroform solution (**1**, 2.77×10^{-4} M; **2**, 2.3×10^{-4} M; **3**, 1.86×10^{-4} M) at 1.064 and 1.907 μm fundamental wavelengths. The former one was emitted by a Q-switched Nd:YAG laser, whereas the latter was obtained by shifting the 1.064 μm emission in a high-pressure hydrogen cell (60 bar). Peak powers of 3.9×10^5 W (at $\lambda = 1.064$ μm) and 5.2×10^5 W (at $\lambda = 1.9$ μm) were achieved with pulses of 10 ns duration and 10 Hz repetition rate. Peak intensities were $\sim 10^{11}$ W/cm^2. A liquid cell with thick windows in the wedge configuration was used to measure the Maker fringes pattern.

The incident beam was synchronized with a DC voltage (4 kV/mm) applied to the solution in order to break its centrosymmetry.

HRS Measurements. The HRS experiments were carried out by measuring the intensity of the scattered second-harmonic light generated when focusing the intense 1.064 μm laser beam on the solution. No indication of multiphoton-induced luminescence was obtained from our experiments.

Theoretical Calculations

The Zn derivatives of the push−pull unsymmetrically substituted alkynyl phthalocyanines studied in this paper were calculated at the semiempirical level. First, geometry optimizations were carried out for all the considered compounds, and second, single-point calculations were performed over the optimized geometries. The single-point calculations were accomplished for characterizing the electronic structure of the compounds and for predicting the electronic UV−visible spectra. Although the unsubstituted ZnPc has been the subject of multiple and (even) high-level theoretical and experimental searches,[21] we have performed some calculations on this molecule to consider the effect of the peripheral substitution on the geometry and electronic properties of the studied compounds. The results of the calculations related to ZnPc have been used in the text only when the comparison was needed.

The structures were optimized using the PM3 method[22] implemented in the MOPAC program package (version 6.0).[23] The geometry optimization procedure employed was the "eigenvector following" (EF).[24] The optimization threshold for the value of gradient norm was fixed to 0.01 kcal/mol (Å or radians). The maximum step size allowed during the optimization procedure was 0.02 (Å or radians). Owing to the relative freedom of orientation of the peripheral $-OC_4H_9$ and $-SO_2C_3H_7$ chains, the hypersurface of potential energy for these compounds may have multiple minima. We made a preliminary study of this surface finding the possible absolute minimum for the studied compounds. The absolute minima obtained for compounds **1**−**3** were those with heats of formation +43.9, +109.8, and −50.9 kcal mol^{-1}, respectively. Energy differences of 12.2, 10.2, and 22.2 kcal mol^{-1} between the global and the other local minima were computed, respectively.

The study of the electronic properties and UV−visible spectra (single-point calculation) was performed with the ZINDO/S[25] method instrumented in the HyperChem (version 5.1)[26] graphic interface. Configuration interaction (CI) was included in the simulation of the spectra. The CI calculations were limited to the six highest occupied and to the six lowest unoccupied molecular orbitals, having in mind that the two highest occupied (HOMOs) and the two lowest unoccupied (LUMOs) molecular orbitals are responsible for the two main bands of the UV−visible spectra in porphyrin-like macrocycles (the Q and B bands),[27] whereas the molecular orbitals nearest in energy can interact with them.[28]

Results and Discussion

Molecular and Electronic Structures. One of the most outstanding geometrical outlines of the considered compounds is that in all of the optimized structures the phthalocyanine skeleton is invariably flat. This result may be understood on the basis of the following:[29] (i) the presence of the Zn atoms in the center of the macrocycle cavity, where zinc optimizes the relationship between the macrocycle cavity and the metal (which is housed in this cavity) sizes; (ii) the benzene rings condensed to the pyrrole ones contribute to the planarity of macrocycle tetrapyrrolic assemblies; and (iii) the phthalocyanine macrocycle is more rigid than the porphyrin one (where the peripheral substitution induces nonplanar conformations of the macrocycle) due to the existence of nitrogens atoms in meso positions.

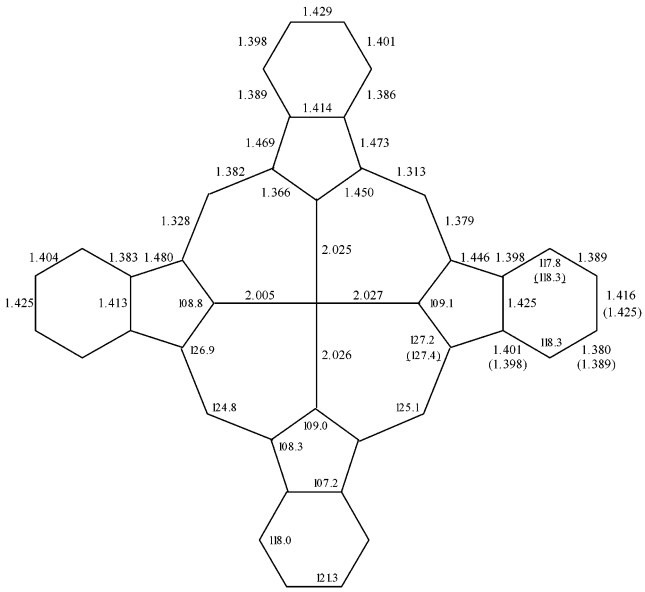

Figure 1. Some selected bond distances (in Å) and angles (in degrees) for the optimized geometries of compounds **1** and **2**. The values into parenthesis correspond to compound **2**.

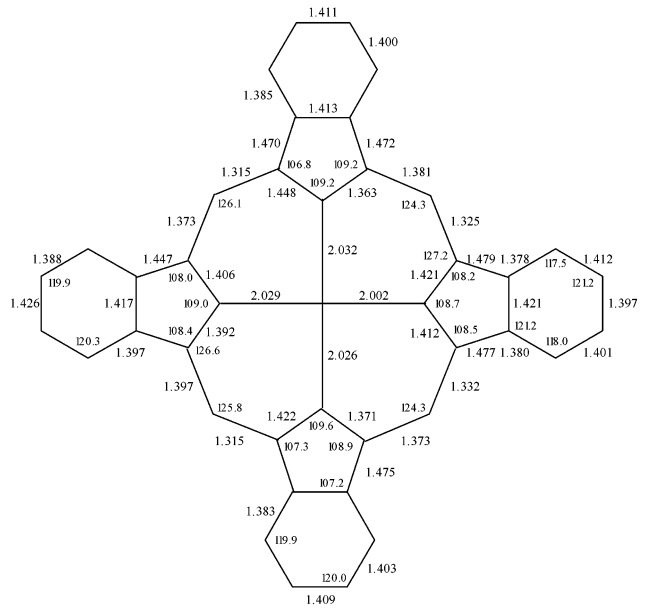

Figure 2. Some selected bond distances (in Å) and angles (in degrees) for the optimized geometry of compound **3**.

Figures 1 and 2 show the optimized geometrical parameters of the macrocycle skeleton for the studied compounds. As it may be observed, the D_{4h} symmetry is broken by the considered peripheral substitution. Two schemes of asymmetry can be distinguished depending on the nature of the substitution pattern: compounds **1** and **2** belong to the first of these schemes, whereas compound **3** conforms to the second one. Furthermore, the degree of the symmetry distortion depends on the presence of one or two electron-withdrawing and electron-donor groups. The 4-nitrophenylethynyl and 4-(dimethylamino)phenylethynyl moieties are always coplanar with the macrocycle structure thus favoring the extension of the π conjugation.

Table 1 contains the calculated ZINDO/S total dipole moments and their components along the "*z*" and "*x*" directions

TABLE 1: Calculated (ZINDO/S) Permanent Dipole Moments (Ground State)

compound	dipole moment/Debye		
	μ_z	μ_x	μ_{total}
1	−12.3	−3.65	12.8
2	−20.6	−0.07	20.6
3	17.1	0.55	17.1

TABLE 2: Calculated ZINDO/S Orbital Energies (in eV) of the Highest Occupied and the Lowest Unoccupied Molecular Orbitals for the Studied Compounds[a]

orbitals	compounds			
	ZnPc	**1**	**2**	**3**
L + 1	−1.72 (e_g)	−1.70	−1.82	−2.56
L	−1.72 (e_g)	−1.86	−2.02	−2.65
H	−5.40 (a_{1u})	−5.60	−5.76	−6.47
H − 1	−8.52 (a_{2u})	−7.79	−7.68	−7.79
H − 2	−8.78 (b_{1u})	−8.13	−8.27	−8.99

[a] For comparison the orbital energies of the unsubstituted ZnPc are included.

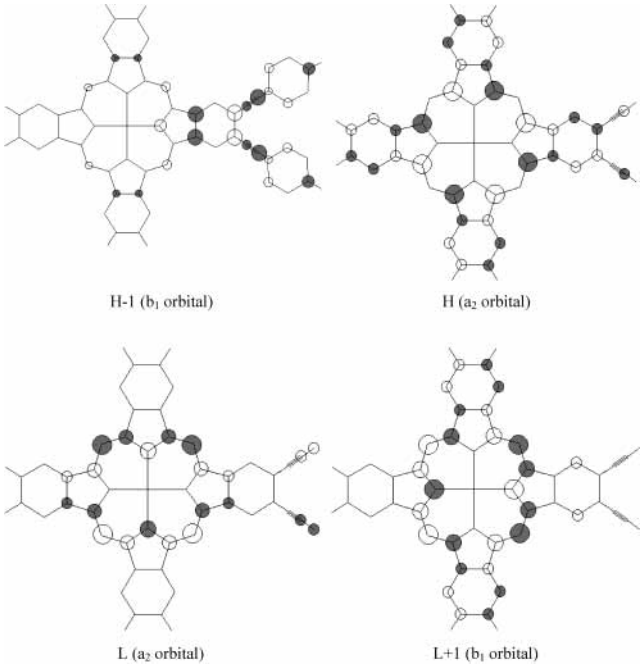

Figure 3. Atomic orbital contributions both to the highest occupied (HOMOs) and the two lowest unoccupied (LUMOs) molecular orbitals for compound **2**. The orbital symmetry is indicated.

(shown in Chart 1) for compounds **1**−**3**. A predominant contribution of the μ_z component to the total dipole moment is observed, i.e., of the component of the "*z*" axis along which the electron-donor (or electron-acceptor) substituent group is placed. The dipole moment component in the "*y*" direction (the direction perpendicular to the plane that contains the molecule skeleton) is zero for all of the studied cases because the $-OC_4H_9$ and $-SO_2C_3H_7$ groups are located either in the plane of the molecule (compounds **1** and **2**) or alternatively above and below the molecular plane in compound **3**. The sign of the μ_z component is in accordance with the electron-donor or electron-acceptor nature of the push−pull group.

Table 2 includes the ZINDO/S calculated orbital energies in the vicinity of the frontier orbitals (HOMOs and LUMOs) for the present compounds, whereas Figures 3 and 4 show the nodal patterns, both of the two highest occupied and the two lowest unoccupied molecular orbitals in compounds **2** and **3**, respectively. The color of the circle indicates the sign of the coefficient C_i where $C_i = \sum c_i$, (c_i are the coefficients of the atomic orbitals in the expression for the molecular orbital) whereas the diameter of the circles is proportional to the absolute value of C_i. C_i was calculated for each atom of the molecule, but Figures 3 and 4 only contain those contributions for which $C_i > 0.2$. The corresponding picture for compound **1** is similar to that obtained for compound **2** but distorted by the molecular asymmetry with respect to the "z" axis. The orbital energies of compound **3** are more negative (see Table 2) than those obtained for compounds **1** and **2**. This result may be explained considering the electron acceptor character of the $-SO_2C_3H_7$ substituents.

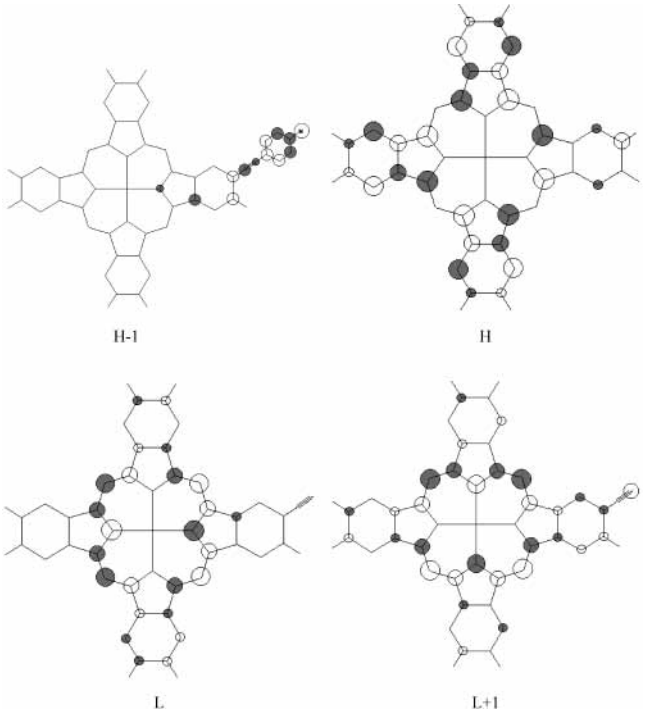

Figure 4. Atomic orbital contributions both to the highest occupied (HOMOs) and the two lowest unoccupied (LUMOs) molecular orbitals for compound **3**.

It is noteworthy that the frontier orbitals in the studied compounds are extensively diffused over the whole macrocyclic structure as may be derived from Figures 3 and 4. Therefore, the HOMOs which are mainly located on the *alpha* carbons (see the nomenclature introduced in the Chart 1), as it is expected for tetrapyrrole macrocycles, also exhibit considerable contributions from the *beta* and *phenyl* carbons. Likewise the LUMOs are extended over the macrocycle structure but they are alternatively distributed along the "*z*" and "*x*" directions. Important contributions to the LUMOs were additionally calculated both on the $-NO_2$ and $-N(CH_3)_2$ substituents. The (HOMO-1)s are not located over the macrocycle but on the $-N(CH_3)_2$ and $-NO_2$ substituents.

As a rule, the HOMOs and LUMOs are located over the planar part of the molecules for all of the studied compounds. Therefore, they are invariably constituted by "p_y" atomic orbitals (see the axis orientation adopted in Chart 1); that is, they have π character, and correspondingly, the electronic transitions among them are always $\pi \rightarrow \pi^*$.

Electronic Transitions: Optical Absorption Spectra. The absorption spectra of the three compounds in chloroform solution (**1**, 2.5×10^{-6} M; **2**, 3.0×10^{-6} M; **3**, 3.6×10^{-6} M) as well as the calculated electronic transitions (represented by vertical lines) are shown in Figure 5. They display the typical

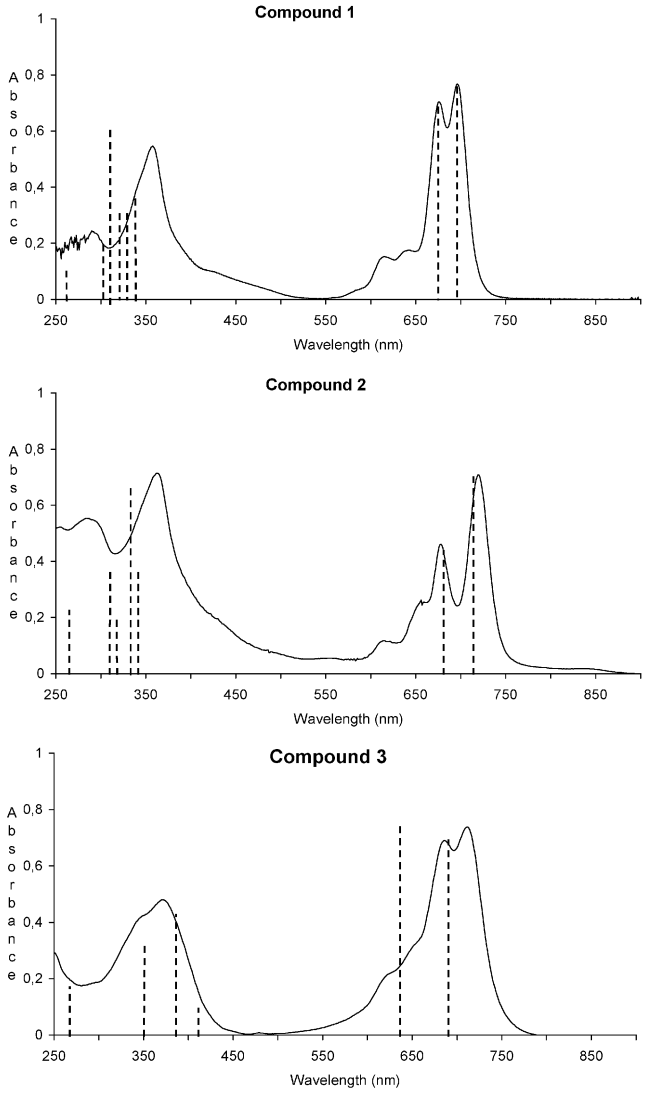

Figure 5. Electronic spectra of compounds **1**, **2** and **3**: experimental data (solid line) and calculated transitions (dotted line).

B and Q features of Pcs. However, because of the breaking of the D_{4h} symmetry induced by the peripheral substitution, the Q-band appears clearly split. Along with this, the observed red shift in the Q-band in compounds **1** and **2** with respect to their precursors[15,16] (the compounds containing the $-C\equiv CH$ groups) is related to the extension of their π-conjugation systems. As was referred to in the previous section, the electron-donor/(withdrawing) groups are coplanar with the tetrapyrrole macrocycle that concentrates the main contribution to the orbitals determining the spectroscopic properties. This feature allows the extension of the π conjugation in compounds **1** and **2** with respect to those where the push−pull groups are replaced by hydrogen (the precursors).

The experimental values for the λ of maximun absorption corresponding to the main observed bands are included in Table 3, together with the calculated λ for the zero-point vibrational electronic transitions. From this, it may be concluded that theoretical calculations provide a satisfactory approximation to the experimental spectroscopic values, particularly those for the Q (Q_1 and Q_2) transitions of compounds **1** and **2**. A major divergence between the experimental and calculated electronic spectra was observed for compound **3**, particularly with regard to Q transitions. This is presumably related to the presence of S atoms at the peripheral $-SO_2C_3H_7$ substituents. In fact, it

TABLE 3: Calculated ZINDO/S and Experimental Spectroscopic Parameters for the Q and B Transitions

		calculated		experimental	
compd	transition	λ/nm	log ϵ	λ_{max}/nm	log ϵ
1	Q_1 (0 → 1)	697	5.1	696	5.4
	Q_2 (0 → 2)	677	5.0	677	5.4
	B	326	5.1	357	5.2
	B	313	4.5		
2	Q_1 (0 → 1)	702	5.1	713	4.9
	Q_2 (0 → 2)	673	4.9	672	4.8
	B	344	3.8	361	4.9
	B	327	4.9		
3	Q_1 (0 → 1)	687	5.1	711	5.3
	Q_2 (0 → 2)	643	5.1	686	5.3
	B	383	4.8	372	5.1
	B	351	4.4		

has been reported in previous theoretical studies[30−32] that the semiempirical methods based on the NDO approach exhibit difficulties for describing the $\pi \rightarrow \pi^*$ electronic transitions in sulfur-containing compounds. In compound **3**, the sulfur atoms directly interact with the HOMO (which is involved in the Q transitions) throughout the phenyl carbons. On the contrary, the ZINDO/S method describes significantly better the B transition. To understand this result, it must be considered that the HOMO-1 in this compound (see Figure 4) is preferentially located on the $-CC(C_6H_4)N(CH_3)_2$ group and interacts weakly with the S atoms.

The symmetry of the electronic transition for these compounds can be well identified for compound **2** because of its strict C_{2v} symmetry. In fact, the Q-band of most of the unsubstituted Pcs corresponds to an $a_1 \rightarrow e_u$ transition.[3] When the structure is perturbed by the peripheral substitution so that the D_{4h} symmetry is turned into the C_{2v} one, the ground orbital becomes a_2 and the degeneracy of the e_u orbitals is broken into a_2 and b_1. Consequently, the orbital energies are reordered. Now the two split Q_1 and Q_2 transitions associated to the Q-band are $a_2 \rightarrow a_2$ appearing at lower energy and $a_2 \rightarrow b_1$ at higher energy. They, respectively, present transition moments parallel to the "*z*" binary axis (Q_1 band) and perpendicular to it (Q_2 band), i.e., along the "*x*" axis. Moreover, these two split transitions have similar strengths and account for the two resolved peaks in the spectra of compound **2**. The components of the transition dipole moments for the Q (Q_1 and Q_2) and B (B_1 and B_2) transitions are given in Table 4. The corresponding values for the transition between the two Q-band excited states are also included. This transition is not observed in the absorption spectra but plays a role in the three-level model calculations of the NLO response to be described below. The situation is more complicated for molecules **1** and **3** because the point symmetry is not C_{2v} and the two transitions may have a mixed ("*z*" and "*x*") character which can be inferred from the corresponding data shown in Table 4.

The Q transitions for the studied compounds are very intense as expected for charge-transfer electronic transitions. The fractions of electronic charge transferred by the Q transitions are 0.28, 0.30, 0.35, and 0.37 for ZnPc and compounds **1**−**3**, respectively. These values were obtained at the semiempirical ZINDO/S level from the atomic charges of the ground and the excited states. The charge transfers for compounds **1**−**3** are approximately in the same range of values and greater than that obtained for ZnPc indicating that (i) the electronic excitations are roughly similar in extension in the studied asymmetric compounds and (ii) their extensions are strongly determined by the push−pull substituents, i.e., the $-NO_2$ and $-N(CH_3)_2$ substituents exert an important influence on the charge transfer

TABLE 4: Calculated (ZINDO/S) Dipole Moments (and Their Components; in Debyes) for the Optical Electronic Transitions and Permanent Dipole Moments of the Excited States Corresponding[a]

		transition dipole			excited-state dipole		
compd	transition	μ_z	μ_x	μ_{total}	μ_z	μ_x	μ_{total}
1	Q_1 (0→1)	−13.2	1.96	13.2	−1.56	−5.71	5.92
	Q_2 (0→2)	2.50	11.6	11.9	−5.60	−1.96	5.93
	B	6.20	6.36	8.88	−14.8	−12.5	19.4
	B	−4.08	2.38	4.72	12.4	1.85	12.5
	1 → 2	7.56	−1.95	17.7			
2	Q_1 (0→1)	−13.9	−0.09	13.9	−9.14	0.02	9.14
	Q_2 (0→2)	0.08	−11.2	11.2	−13.4	−0.02	13.4
	B	0.00	−2.27	2.27	−12.4	−0.01	12.4
	B	−7.75	−0.02	7.75	−10.3	0.03	10.3
	1 → 2	18.3	0.13	18.3			
3	Q_1 (0→1)	-2.58	12.9	13.1	10.2	3.88	10.9
	Q_2 (0→2)	12.8	2.77	13.1	6.17	−0.77	6.22
	B	−4.20	−5.95	7.28	44.6	8.15	45.3
	B	−4.23	0.79	4.30	56.4	7.33	56.9
	1 → 2	−4.19	14.3	14.9			

[a] The assignments correspond by the same order with these utilized in Table 3. In bold are given the electric dipole moments for the electronic transition (1−2) between the two lowest excited states.

TABLE 5: Experimental Results for γ ($\times 10^{-33}$ esu) and β ($\times 10^{-30}$ esu)

compd	μ (D)	γ_{EFISH}[a]	γ_{EFISH}[b]	β_{EFISH}[a]	β_{EFISH}[b]	β_{HRS}[a]
1	12.8	−10.1	2.56	−162	41.1	220
2	20.6	−38.5	52.3	−384	522	530
3	17.1	7.21	−2.13	86.7	−25.6	114

[a] At 1.06 μm. [b] At 1.9 μm.

extension. The peripheral susbstituents do not participate directly in the electronic transfer associated with the Q transition but they quantitatively modulate it. The situation is markedly different for the B transition because the substituents directly contribute to the HOMO-1 (Figures 4 and 5).

The highest charge changes (for Q transitions) were observed on the alpha carbons, with the meso and pyrrole nitrogens being positive for the former and negative for the last ones. This means that the Q electronic transitions occur from the alpha carbons to the nitrogens in correspondence with the spatial distribution of the HOMO and LUMOs (Figures 4 and 5).

NLO Properties. The γ(EFISH) values measured at 1.064 and 1.907 μm and β(HRS) values at 1.064 μm are listed in Table 5. The β(HRS) data indicate that molecule **2** (exhibiting the highest degree of asymmetry) reaches the largest SHG response. For the other compounds, the β(HRS) values are substantially lower. Although HRS data are not available for other asymmetric Pcs, our molecules present superior EFISH performances to those measured for analogous push−pull Pcs not having an ethynediyl moiety in the linking bridge.[16] Moreover, values are comparable to those reported for highly efficient SubPcs where thorough experimental investigations have been carried out.[6a] The detailed quantitative analysis of γ(EFISH) data, presenting opposite signs at 1.064 and 1.904 μm, is more complicated. In principle, one may ignore the electronic contribution to gamma EFISH as often done and calculate β(EFISH) from the simple equation:

$$\gamma(\text{EFISH}) = \mu \cdot \beta(\text{EFISH})/5kT \qquad (1)$$

The corresponding β(EFISH) values are listed in Table 5. They are, also, quite significant and much larger than those measured for analogous noncentrosymmetric Pcs, lacking the triple bond in the bridge connecting the acceptor and donor moieties. Moreover, the trend found for the absolute values on passing from compound **1** to **3** is consistent with that found for the HRS data; that is, values decrease with the sequence **2** → **1** → **3**. Unfortunately, expression 1 does not include the electronic contribution to γ_{EFISH} and cannot therefore be considered as fully reliable for strongly conjugated molecules as those investigated in this work. Therefore, a theoretical evaluation of all components of the beta tensor has been carried out for compound **2**, using a three-level model and the molecular parameters calculated in the above section. Because molecule **2** strictly abides to C_{2v} symmetry, theoretical formulas for β_{ijk} are relatively simple and manageable. From those, tensor components of β_{EFISH} have been readily obtained. The value is higher than that obtained from the simple formula 1, ignoring electronic contributions, and it is expected to be more meaningful. Moreover, β_{HRS} has been also determined and compared to the experimental value.

Theoretical Three-Level Model. The spectral data suggest that for compound **2**, displaying strict C_{2v} symmetry, a three-level model including the two excited levels responsible for the Q peaks and the ground level may be appropriate and meaningful. It has also been shown by general symmetry arguments that a 2-dimensional C_{2v} molecule requires a three-level system to be able to sustain a β tensor with both nonvanishing β_{zzz} and β_{zxx} components.[2f] To simplify the mathematical expressions, we will adopt the nomenclature: 0 for the ground state, 1 for the a_2 excited state, and 2 for the b_1 excited state. For a planar molecule with that point symmetry, the three-level expressions for the three nonzero components of the hyperpolarizability tensor (β_{zzz}, β_{zxx}, and β_{xxz}) are

$$\beta_{zzz} = \frac{1}{\hbar^2}[(\mu^z_{01})^2 \Delta\mu^z_{01}(2D^a_{11} + D^b_{11})]$$

$$\beta_{zxx} = \frac{1}{\hbar^2}[(\mu^x_{02})^2 \Delta\mu^z_{02} D^b_{22} + 2\mu^z_{01}\mu^x_{02}\mu^x_{12} D^a_{12}] \qquad (2)$$

$$\beta_{xxz} = \frac{1}{\hbar^2}[(\mu^x_{02})^2 \Delta\mu^z_{02} D^a_{22} + \mu^x_{02}\mu^x_{12}\mu^z_{01}(D^a_{21} + D^b_{12})]$$

where $\mu^{x,y,z}_{i,j}$ stands for the x,y,z components of the optical transition moment between levels i and j and $\Delta\mu^{x,y,z}_{ij} = \mu^{x,y,z}_j - \mu^{x,y,z}_i$ represents the components of the change in permanent dipole moment from level i to level j.

In terms of the tensor components (2), the EFISH and HRS hyperpolarizabilities are given by

$$\beta_{(\text{EFISH})} = \frac{1}{\hbar^2}\Big\{(\mu^z_{01})^2 \Delta\mu^z_{01}(2D^a_{11} + D^b_{11}) + \frac{1}{3}[(\mu^x_{02})^2 \Delta\mu^z_{02} (2D^a_{22} + D^b_{22}) + 2\mu^z_{01}\mu^x_{02}\mu^x_{12}(D^a_{12} + D^a_{21} + D^b_{12})]\Big\} \qquad (3)$$

and

$$\beta_{(\text{HRS})} = \frac{6}{35}\beta^2_{zzz} + \frac{2}{21}\beta_{zzz}\beta_{zxx} + \frac{4}{35}\beta^2_{zxx} + \frac{2}{35}\beta_{zzz}\beta_{xxz} + \frac{20}{105}\beta^2_{xxz} + \frac{2}{35}\beta_{zxx}\beta_{xxz} \qquad (4)$$

Note that Kleimann symmetry has not been assumed. This is a relevant point because one of the wavelengths used in this work (1.064 μm) is partly resonant at the harmonic frequency.

TABLE 6: Theoretical Results for β ($\times 10^{-30}$ esu) of Compound 2

μ_{12} (D)	$\beta_{zzz}{}^a$	$\beta_{zxx}{}^a$	$\beta_{xxz}{}^a$	$\beta_{\mathrm{HRS}}{}^a$	$\beta_{\mathrm{EFISH}}{}^a$	$\beta_{\mathrm{EFISH}}{}^b$
18.3	−975	286	−881	573	−2009	2095
0	−975	−259	−211	467	−1119	1246

[a] At 1.06 μm. [b] At 1.9 μm.

The dispersive factors used so far are given by the following expressions:

$$2D_{ii}^{a} + D_{ii}^{b} = \frac{3\omega_{0i}{}^2}{2(\omega_{0i}{}^2 - 4\omega^2)(\omega_{0i}{}^2 - \omega^2)}$$

$$D_{22}^{a} = \frac{\omega_{0i}{}^2 + 2\omega^2}{2(\omega_{0i}{}^2 - 4\omega^2)(\omega_{0i}{}^2 - \omega^2)}$$

$$D_{22}^{b} = \frac{1}{2(\omega_{0i}{}^2 - \omega^2)}$$

$$D_{12}^{a} + D_{21}^{a} + D_{12}^{b} = \frac{\omega_{01}\omega_{02} + 2\omega^2}{2(\omega_{01}{}^2 - 4\omega^2)(\omega_{02}{}^2 - \omega^2)} + \frac{\omega_{01}\omega_{02} + 2\omega^2}{2(\omega_{02}{}^2 - 4\omega^2)(\omega_{01}{}^2 - \omega^2)} + \frac{\omega_{01}\omega_{02} + 2\omega^2}{2(\omega_{01}{}^2 - \omega^2)(\omega_{02}{}^2 - \omega^2)} \quad (5)$$

where D_{12}^{a} is the first term, D_{21}^{a} is the second term, and D_{12}^{b} is the third term on the right hand side of eq 5. The transition moments appearing in the above expressions are derived from the area of the corresponding absorption bands,[33] which are in very good agreement with those theoretically calculated. On the other hand, for the permanent dipole moments of the ground and the two excited states, one may use the (in-plane) theoretical values given in Table 1. The transition moment μ_{12} between the two lowest excited levels, which is not experimentally available, is taken from Table 4. Values obtained for all nonzero components of the β tensor are given in Table 6. For comparison the results obtained ignoring the **1** → **2** transition, i.e., taking $\mu_{12} = 0$, are also included. One observes that β_{zzz} is highest as expected for the push−pull character of the molecule and quite significant in comparison with related compounds.[4] However, the off-diagonal elements β_{zxx} and β_{xxz} are quite high and even comparable to β_{zzz} in accordance with the 2-D structure of our molecules. Moreover, at variance with the diagonal component, they are very sensitive to the transition dipole moment μ_{12}. The calculated β_{ijk} values have been, then, introduced in the expressions for β_{EFISH} and β_{HRS}, and the obtained results are also included in Table 6. One, first, observes that the β_{EFISH} results very largely differ from those obtained by using the simple expression 1 that ignores the electronic contributions to γ_{EFISH}. This is a confirmation of the relative importance of these contributions for highly conjugated molecules.[17] Moreover, within this theoretical framework, the opposite signs for the β_{EFISH} data at 1.064 and 1.907 μm derive from the different dispersion factors and account for the different signs of γ_{EFISH} at those wavelengths. As for β_{HRS}, the accordance between the theoretically predicted and experimental values can be considered excellent because of the approximations of the model, and it provides strong support for our analysis. One should realize that the method does not involve the fitting of any parameter. The agreement might be possibly improved by using a more elaborate model including damping effects and additional levels but this might significantly and unnecessarily increase the mathematical complexity at the expense of clarity.

The model assuming strict, either Z or X transition moments, for the two peaks observed at the Q-band region is not expected to apply for compounds **1** and **3**. However, one may still assume approximate C_{2v} symmetry and use the same formalism. Results for β_{EFISH} and β_{HRS} are not reliable, and so they are not given here. However, they confirm the trends illustrated in Table 5, although the quantitative concordance is now much poorer, standing out the important role of symmetry.

Conclusions

A detailed theoretical and experimental study of the electronic and optical (linear and nonlinear) properties of a new family of peripherally substituted push−pull phthalocyanines, having electron-donor and strong electron-withdrawing substituents, has been carried out.

The studied compounds preserve the planarity of the phthalocyanine macrocycle, which is shown to extend to the electron-donor or electron-withdrawing substituents, thus increasing the π conjugation of the system. Peripheral substitution induces a breakdown of the molecular D_{4h} symmetry of the ZnPc and determines both the splitting of the Q electronic transitions and their symmetry.

HOMOs and LUMOs are located on the planar phthalocyanine fragment whereas the (LUMO-1)s, as opposed to most of the tetrapyrrole macrocyclic compounds, exhibiting strong localization on the electron-donor/(acceptor) substituents. Even if the electron-donor/(acceptor) substituents do not participate directly in the Q electronic transition, they modulate both the extension and the direction of the charge transfer. They also determine the orientation of the electronic dipole moment both in the excited and ground state.

As for the NLO behavior, significant SHG hyperpolarizabilities have been measured through EFISH and HRS. Values are the largest found for push−pull Pcs and offer a route for optimization of the SHG response and related properties such as electrooptic efficiency. The data have been analyzed with a three-level model and a C_{2v} geometry, and both diagonal and off-diagonal components of the beta tensor have been determined. The parameters used in the expressions for the molecular hyperpolarizabilities have been obtained from ZINDO/S calculations of molecular orbital and electric transition moments on optimized molecular geometries. These calculations provide an excellent fitting to the experimental spectroscopic data and satisfactorily account for the HRS hyperpolarizability of compound **2** having C_{2v} symmetry.

Acknowledgment. CICYT (Spain), Ministerio de Educación y Cultura (Spain), Comunidad de Madrid (Spain), and the European Union through Grants BQU2002-04697, PB97-0027, PB98-0061, SAB1998-0165, 07N/0030/2002, and HPRN-CT-2000-00020 supported this work, respectively.

References and Notes

(1) (a) Brédas, J. L.; Adant, C.; Tackx, P.; Persoons, A. *Chem. Rev.* **1994**, *94*, 243. (b) Brédas, J. L.; Cornill, J.; Beljonne, D.; dos Santos, D. A.; Shuai, Z. *Acc. Chem. Res*. **1999**, *32*, 267. (c) Kanis, D. R.; Ratner, M. A.; Marks, T. J. *Chem. Rev.* **1994**, *94*, 195. (d) *Nonlinear Optical Properties of Organic Molecules and Crystals*; Zyss, J., Chemla, D. S., Eds.; Academic Press: New York, 1987; Vols. 1 and 2.

(2) (a) Zyss, J. *Nonlinear Opt.* **1991**, *1*, 3. (b) Zyss, J. *J. Chem. Phys*. **1993**, *98*, 6583. (c) Yaron, D.; Joffre, M.; Zyss, J.; Silbey, R. *J. Chem. Phys.* **1992**, *97*, 5607. (d) Zyss, J.; Ledoux, I. *Chem. Rev.* **1994**, *94*, 77. (e) Brasselet, S.; Zyss, J. *J. Opt. Soc. Am. B* **1998**, *15*, 257. (f) Zyss, J.; Brasselet, S. *Opt. Phys*. **1998**, *7*, 397. (g) Wong, M. S.; Bosshard, C.; Pan, F.; Günter,

P. *Adv. Mater*. **1996**, *8*, 677. (h) Maslak, P.; Chopra, A.; Moylom, C. R.; Wortmann, R.; Lebus, S.; Rheingold, A. L.; Yap, G. A. P. *J. Am. Chem. Soc.* **1996**, *118*, 1471. (i) García-Martínez, A.; Barcina, J. V.; De Fresno-Cerezo, A.; Rojo, G.; Agulló-López, F. *J. Phys. Chem. B* **2000**, *104*, 43.

(3) (a) *Phthalocyanines. Properties and Applications*; Leznoff, C. C., Lever, A. B. P., Eds.; VCH Publishers (LSK) Ltd.: Cambridge, 1989, 1993, 1996; Vols. 1−4. (b) Hanack, M.; Heckmann, H.; Polley, R. *Methods in Organic Chemistry* (Houben-Weyl); Schaumann, E., Ed.; Georg Thieme Verlag: Stuttgart, Germany, 1998; Vol. E 9d, pp 717−833. (c) Mckeown, N. B. *Phthalocyanines Materials, Synthesis, Structure and Function*; Cambridge University Press: Cambridge, 1998. (d) De la Torre, G.; Nicolau, M.; Torres, T. *Supramolecular Photosensitive and Electroactive Materials*; Nalwa, H. S., Ed.; Academic Press: New York, 2001; p 1−111.

(4) For reviews on the NLO properties of Pcs, see: (a) Nalwa, H. S.; Miyata, S. *Nonlinear Optics of Organic Molecules and Polymers*; CRC Press: Boca Raton, FL, 1997. (b) De la Torre, G.; Torres, T.; Agulló-López, F. *Adv. Mater*. **1997**, *9*, 265. (c) De la Torre, G.; Vázquez, P.; Agulló-López, F.; Torres, T. *J. Mater. Chem*. **1998**, *8*, 1671. (d) Dini, D.; Barthel, M.; Hanack, M. *Eur. Joc. Chem*. **2001**, 3759. (e) Hanack, M.; Schneider, T.; Barthel, M.; Shirk, J. S.; Flom, S. R.; Pong, R.-G. S. *Coord. Chem. Rev*. **2001**, *219*−*221*, 235.

(5) Rojo, G.; Agulló-López, F.; Cabezón, B.; Torres, T.; Brasselet, S.; Ledoux, I.; Zyss, J. *J. Phys. Chem. B* **2000**, *104*, 4295.

(6) (a) Del Rey, B.; Keller, U.; Torres, T.; Rojo, G.; Agulló-López, F.; Nonell, S.; Martí, C.; Brasselet, S.; Ledoux, I.; Zyss, J. *J. Am. Chem. Soc*. **1998**, *120*, 12808. (b) Claessens, C.; Torres, T. *Chem. Eur. J*. **2000**, *6*, 2168.

(7) Rojo, G.; Martín, G.; Agulló-López, F.; Torres, T.; Heckmann, H.; Hanack, M. *J. Phys. Chem. B* **2000**, *104*, 7066.

(8) Fox, J. M.; Katz, T. J.; Elshocht, S. V.; Verbiest, T.; Kauranen, M.; Persoons, A.; Thongpanchang, T. T.; Krauss, T.; Brus, L. *J. Am. Chem. Soc*. **1999**, *121*, 3453.

(9) (a) Li, D. A.; Ratner, M. A.; Marks, T. J. *J. Am. Chem. Soc.* **1988**, *110*, 1707. (b) Li, D.; Marks, T. J.; Ratner, M. A. *Chem. Phys. Lett*. **1986**, *131*, 370.

(10) (a) Liu, Y.; Xu, Y.; Zhu, D.; Wada, T.; Sasabe, H.; Liu, L.; Wang, W. *Thin Solid Films* **1994**, *244*, 943. (b) Liu, Y.; Xu, Y.; Zhu, D.; Wada, T.; Sasabe, H.; Zhao, X.; Xie, X. *J. Phys. Chem.* **1995**, *99*, 6957. (c) Liu, Y.; Xu, Y.; Zhu, D.; Zhao, X. *Thin Solid Films* **1996**, *289*, 282. (d) Liu, S. G.; Liu, Y.-Q.; Xu, Y.; Zhu, D.-B.; Yu, A.-C.; Zhao, X.-S. *Langmuir* **1998**, *14*, 690.

(11) (a) Díaz-García, M. A.; Agulló-López, F.; Sastre, A.; Del Rey, B.; Torres, T.; Dhenaut, C.; Ledoux, I.; Zyss, J. *MCLC S&T Sect. B: Nonlinear Opt.* **1996**, *15*, 251. (b) Sastre, A.; Díaz-García, M. A.; Del Rey, B.; Dhenaut, C.; Zyss, J.; Ledoux, I.; Agulló-López, F.; Torres, T. *J. Phys. Chem.* **1997**, *101*, 9773.

(12) (a) Tian, M.; Wada, T.; Sasabe, H. J. *Heterocyclic Chem*. **1997**, *34*, 171. (b) Tian, M.; Wada, T.; Kimura-Suda, H.; Sasabe, H. *Mol. Cryst. Liq. Cryst*. **1997**, *294*, 271. (c) Tian, M.; Wada, T.; Kimura-Suda, H.; Sasabe, H. *J. Mater. Chem*. **1997**, *7*, 861.

(13) LeCours, S. M.; Guan, H.-W.; DiMagno, S. G.; Wang, C. H.; Therien, M. J. *J. Am. Chem. Soc.* **1996**, *118*, 1497.

(14) Priyadarshy, S.; Therien, M. J.; Beratan, D. N. *J. Am. Chem. Soc.* **1996**, *118*, 1504.

(15) The synthesis of these compounds has been described previously: Maya, E. M.; García, C.; García-Frutos, E. M.; Vázquez, P.; Torres, T. *J. Org. Chem*. **2000**, *65*, 2733.

(16) For recent examples of alkynyl substituted phthalocyanines, see: (a) Maya, E. M.; Vázquez, P.; Torres, T. *Chem. Eur. J*. **1999**, *5*, 2004. (b) García-Frutos, E. M.; Fernández-Lázaro, F.; Maya, E. M.; Vázquez; P.; Torres, T. *J. Org. Chem*. **2000**, *65*, 6841.

(17) Rojo, G.; De la Torre, G.; García-Ruiz, J.; Ledoux, I.; Zyss, J.; Torres, T.; Agulló-López, F. *Chem. Phys*. **1999**, *245*, 27.

(18) (a) Therune, R. W.; Maker, P. D.; Savage, C. D. *Phys. Rev. Lett*. **1965**, *14*, 681. (b) Maker, P. D. *Phys. Rev. A* **1970**, *1*, 923. (c) Clays, K.; Persoons, A. *Phys. Rev. Lett*. **1991**, *66*, 2980 and references 2d and 2e above.

(19) (a) Levine, B. F.; Bethea, C. G. *J. Chem. Phys*. **1975**, *63* (5), 2666. (b) Oudar, J. L.; Chemla, D. S. *J. Chem. Phys*. **1977**, *66* (6), 2664. (c) Ledoux, I.; Zyss, J. *Chem. Phys*. **1982**, *73*, 203.

(20) Reference 2b and Brasselet, S.; Zyss, J. *J. Nonlinear Opt. Phys*. **1996**, *5*, 671.

(21) (a) Laemon, D.; Parrinello, M. *Chem. Phys. Lett*. **1994**, *116*, 1932. (b) Engel, M. K. *Rep. Kawamura Inst. Chem. Res*. **1997**, *1996*, 11. (c) Piet, D. P.; Danovich, D.; Zuilhof, H.; Sudhölter, E. J. R. *J. Chem. Soc., Perkin Trans. 2* **1999**, *8*, 1653. (d) Hashimoto, T.; Choe, Y.-K.; Nakano, H.; Hirao, K. *J. Phys. Chem. A* **1999**, *103*, 1894.

(22) (a) Stewart, J. J. P. *J. Comput. Chem*. **1989**, *10*, 209. (b) Stewart, J. J. P. *J. Comput. Chem*. **1989**, *10*, 221.

(23) Stewart, J. J. P. *J. Computer-Aided Mol. Design* **1990**, *4*, 1.

(24) Baker, J. *J. Comput. Chem*. **1986**, *7*, 385.

(25) Anderson, P.; Edwards, M.; Zerner, M. C. *Inor. Chem*. **1986**, *28*, 2728.

(26) *HyperChem 5.11*; Hypercube, Inc., Scientific Software. 1999.

(27) (a) Gouterman, M. *J. Mol. Spectrosc*. **1961**, *6*, 138. (b) Nagashima, U.; Takada, T.; Ohno, K. *J. Chem. Phys*. **1986**, *85*, 4524−4529. (c) Serrano-Andres, L.; Merchán, M.; Rubio, M.; Roos, B. O. *Chem. Phys. Lett*. **1998**, *295*, 195. (d) Hashimoto, T.; Choe, Y.-K.; Nakano, H.; Hirao, K. *J. Phys. Chem. A* **1999**, *103*, 1894. (e) Rubio, M.; Roos, B. O.; Serrano-Andres, L.; Merchan, M. *J. Chem. Phys*. **1999**, *110*, 7202. (f) Gisbergen, S. J. A.; Rosa, A.; Ricciardi, G.; Baerends, E. J. *J. Chem. Phys*. **1999**, *111*, 2499.

(28) Toyota, K.; Hasegawa, J.; Nakatsuji, H. *Chem. Phys. Lett*. **1996**, *250*, 437.

(29) (a) Poveda, L. A.; Ferro, V. R.; García de la Vega, J. M.; González-Jonte, R. H. *Phys. Chem. Chem. Phys*. **2000**, *2*, 4147 and references therein. (b) Poveda, L. A.; Ferro, V. R.; García de la Vega, J. M.; González-Jonte, R. H. *J. Comp-Aided Mol. Design*. **2001**, *15*, 183.

(30) Ferro, V. R.; Poveda, L. A.; González-Jonte, R. H.; García de la Vega, J. M.; Torres, T.; del Rey, B. J. *Porphyrins Phthalocyanines* **2000**, *4*, 610.

(31) Hedström, M.; Salhi-Benachenhou, N.; Calais, J. L. *Mol. Eng*. **1994**, *3*, 329.

(32) Fabian, J.; Diaz, L. A.; Seifert, G.; Niehaus, T. *J. Mol. Struct. (THEOCHEM)* **2002**, *594*, 41.

(33) Mulliken, R. S. *J. Phys. Chem.* **1939**, *7*, 14.